53rd IEEE Conference on Decision and Control
December 15-17, 2014. Los Angeles, California, USA

Embedding of SLIP Dynamics on Underactuated Bipedal Robots through Multi-Objective Quadratic Program based Control

Ayonga Hereid, Matthew J. Powell, and Aaron D. Ames

Abstract— **This paper presents a method for achieving stable periodic walking, consisting of phases of single and double support, on underactuated walking robots by embedding Spring Loaded Inverted Pendulum (SLIP) dynamics. Beginning with a SLIP model, the dynamics are stabilized to a constant energy level and periodic walking gaits are found; an equality constraint on torque can be used to shape the dynamics of the full-order robot to obey the corresponding SLIP dynamics. To transition these gaits to full-order robots, the essential elements of SLIP walking gaits, i.e., the swing leg touchdown angle, are utilized to synthesis control Lyapunov functions that result in inequality constraints in torque. Finally, the desired force interactions with the environment as dictated by SLIP dynamics are utilized to obtain inequality constraints in the reaction forces. Combining these equality and inequality constraints results in a multi-objective quadratic program based controller that is implemented on a multi-domain hybrid system model of an underactuated bipedal robot. The end result is stable periodic walking on the full-order model that shows remarkable similarity to the SLIP gait from which it was derived.**

I. Introduction

The Spring Loaded Inverted Pendulum (SLIP) model provides a low-dimensional representation of locomotion inspired by biological principles [12], [7]. As a result of this biological motivation, the ability to realize SLIP-like walking gaits on bipedal robots promises to result in natural, efficient and robust locomotion. This is evidenced by the classic work by Raibert on hopping robots [18], which has since motivated the study of walking and running in robotic systems with simple SLIP models [2], [20]. Ultimately, the fundamental limitation in realizing the benefits of SLIP inspired locomotion is the low-dimensional nature of the SLIP model, and the difficulty of realizing this low-dimensional behavior on full-order high-dimensional walking robots.

This paper presents a method for realizing SLIP dynamics directly on full-order underactuated walking robots, modeled as multi-domain hybrid systems, with the end result being the automatic synthesis of stable walking gaits that qualitatively display SLIP-like behavior. This process of embedding SLIP gaits into full-order robotic systems is inherently difficult due to the complexity of the multiple control tasks that must be simultaneously achieved. In particular, the dynamics of the Center of Mass (CoM) of the full-order system must be shaped so as to evolve according to the SLIP dynamics. Additionally, virtual constraints must be synthesized so as to capture the fundamental assumptions of SLIP walking gaits, e.g., a specific touch down angle of the swing leg must be achieved. Finally, the interaction of the robot with the environment (expressed as reaction forces) must be controlled directly to obtain SLIP-like behavior. The difficulty of realizing these ideas on a full-order robot is that they define a large set of control objectives that are difficult to simultaneously achieve—especially in the context of underactuation.

A. Hereid. M. J. Powell, and A. D. Ames are with the Department of Mechanical Engineering, Texas A&M University, College Station, TX 77843, e-mail: {ayonga,mjpowell,aames}@tamu.edu

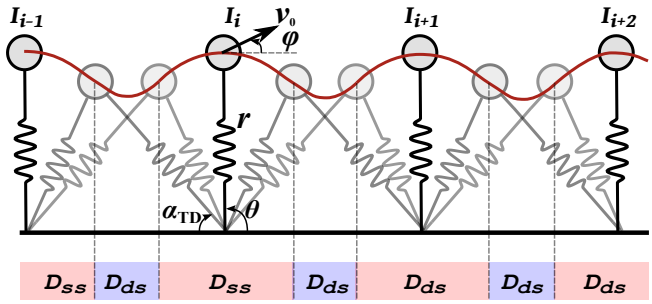

Fig. 1: The Spring Loaded Inverted Pendulum Walking Gait.

In order to balance the multiple control objectives necessary to achieve SLIP-like locomotion on full-order bipedal robots, this paper presents a novel control methodology based upon multi-objective quadratic programs (QP). The role of QPs in the control of walking robots was first studied in [5], where a novel class of control Lyapunov functions (CLFs)—rapidly exponentially stabilizing CLFs—were introduced and shown to guarantee stable walking gaits. The fact that CLFs can be naturally realized as controllers through QPs [9] motivated the use of QPs in the context of walking robots [10]. These ideas were extended in [6], [16] to simultaneously achieve multiple control objectives—expressed through CLFs—together with desired reaction forces. Motivated by these constructions, all of the salient elements of SLIP gaits are encoded as equality and inequality constraints that can be simultaneously achieved via a QP based controller: the dynamics of the COM are shaped to be the dynamics of an energy stabilized SLIP model through equality constraints; virtual constraint based objectives yield inequality constraints through CLFs; and ground reaction forces are regulated to agree with the SLIP model via additional inequality constraints. The end result is a stable walking gait for an underactuated robot, consisting of phases of single and double support, that is directly obtained from an energy stabilized SLIP gait.

Existing work on underactuated dynamic robotic locomotion has successfully utilized the notion of hybrid zero dynamics (HZD); this methodology utilizes the hybrid nature of

walking robots in order to define virtual constraints that are invariant through impacts [22]. HZD has been successfully applied to a large collection of bipedal robots to achieve walking, including MABEL [21], AMBER [3], and the robot of interest in this paper: ATRIAS [19]. Notably, in [14], the authors utilized HZD and human-inspired control [3] to achieve SLIP-inspired locomotion on ATRIAS [1]. While HZD gives formal guarantees on generating stable walking gaits, it requires *a priori* nonlinear optimization to find stable walking gaits; this is time consuming and convergence can be an issue for complex robots. Methodologies from HZD were leveraged to obtain results on formally embedding SLIP dynamics into more complex robots [17] for single-leg hoppers. Only recently has work considered extending SLIP gaits directly to full-order robots [11], yet this was done in the context of full actuation—greatly simplifying the problem—and the hybrid system model of a bipedal robot was not considered. Therefore, this work differentiates itself from existing results in the following notable ways: underactuation is considered, phases of single and double support are utilized and modeled via a multi-domain hybrid system model, and no *a priori* optimization is needed (as in the case of HZD) to generate stable periodic gaits.

II. Robot Model

This section describes the hybrid model of the robot of interest–ATRIAS–in detail. ATRIAS is a human-scale, underactuated bipedal robot built at the Oregon State University Dynamic Robotics Laboratory. Designed to match key characteristics of the SLIP model, ATRIAS places all heavy elements, such as actuators, at the torso and drives lightweight four bar mechanisms on each leg which terminate in point feet through series compliant actuators [13]. This enables ATRIAS to achieve agile, efficient and highly dynamic maneuvers [1]. In this paper, we only consider the rigid part of the robot assuming the joints are directly controlled.

Hybrid System Model. Due to the two different phases of the SLIP walking gait and the discrete dynamics of the system at impacts, the mathematical framework of multi-domain hybrid system is used for this bipedal robot [14]. For walking with point feet, the hybrid model discrete domains are limited to only the *double* and *single* support phase (see Fig. 2).

Considering the configuration space given by the generalized coordinates $q = \{p_x, p_y, q_T, q_{1s}, q_{2s}, q_{1ns}, q_{2ns}\}^T \in \mathcal{Q} \subset \mathbb{R}^2 \times SO(2) \times \mathcal{Q}_b$ with $n = \dim(\mathcal{Q})$, as shown in Fig. 3 (a), the formal hybrid model for the two-domain locomotion is given by the *tuple*:

$$\mathscr{HC} = (\Gamma, \mathcal{D}, \mathcal{U}, S, \Delta, FG), \tag{1}$$

where

- $\Gamma = (V, E)$ is the directed graph specific to this hybrid system, with vertices $V = \{\mathbf{ss}, \mathbf{ds}\}$, where $\mathbf{ss}$ and $\mathbf{ds}$ represent single and double support phases, respectively, and edges $E = \{e_1 = \{\mathbf{ss} \to \mathbf{ds}\}, e_2 = \{\mathbf{ds} \to \mathbf{ss}\}\}$,
- $\mathcal{D} = \{\mathcal{D}_{\mathbf{ss}}, \mathcal{D}_{\mathbf{ds}}\}$ is a set of two domains,

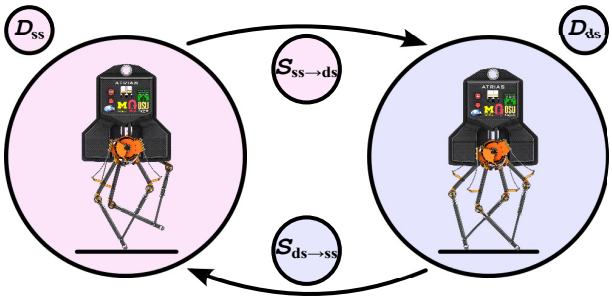

Fig. 2: The directed graph of single/double support phase.

- $\mathcal{U} = \{\mathcal{U}_{\mathbf{ss}}, \mathcal{U}_{\mathbf{ds}}\}$ is a set of admissible controls,
- $S = \{S_{\mathbf{ss}\to\mathbf{ds}}, S_{\mathbf{ds}\to\mathbf{ss}}\}$ is a set of guards,
- $\Delta = \{\Delta_{\mathbf{ss}\to\mathbf{ds}}, \Delta_{\mathbf{ds}\to\mathbf{ss}}\}$ is a set of reset maps,
- $FG = \{(f_{\mathbf{ss}}, g_{\mathbf{ss}}), (f_{\mathbf{ds}}, g_{\mathbf{ds}})\}$ is a control system on each $\mathcal{D}_v$ for $v \in V$.

The two domains $\{\mathcal{D}_{\mathbf{ss}}, \mathcal{D}_{\mathbf{ds}}\}$ are depicted in Fig. 2. The remainder of this section will be focused on how to construct the individual elements of the two-domain hybrid system.

Domains and Guards. In the double support domain, the non-stance foot must remain on the ground. A transition from double support to single support occurs when the normal reaction force on the non-stance foot crosses zero. Therefore, the double support domain and guard are given by:

$$\mathcal{D}_{\mathbf{ds}} = \{(q, \dot{q}, u) : h_{ns}(q) = 0, F^y_{ns}(q, \dot{q}, u) \geq 0\}, \tag{2}$$
$$S_{\mathbf{ds}\to\mathbf{ss}} = \{(q, \dot{q}, u) : h_{ns}(q) = 0, F^y_{ns}(q, \dot{q}, u) = 0\}, \tag{3}$$

where $h_{ns}(q)$ is the height of the non-stance foot, and F^y_{ns} is the normal contact force on the non-stance foot, which will be defined later in the section. Since there is no impact involved for the transition from double support to single support, the states of the robot remain the same. Therefore the reset map from double support to single support is the identity map: $\Delta_{\mathbf{ds}\to\mathbf{ss}} = \mathbf{I}$.

For the single support domain, the non-stance foot is above the ground. When the non-stance foot strikes the ground a guard is reached and the transition to the next domain takes place. Hence, the single support domain and guard has the following structure:

$$\mathcal{D}_{\mathbf{ss}} = \{(q, \dot{q}, u) : h_{ns}(q) \geq 0, F^y_{ns}(q, \dot{q}, u) = 0\}, \tag{4}$$
$$S_{\mathbf{ss}\to\mathbf{ds}} = \{(q, \dot{q}) : h_{ns}(q) = 0, \dot{h}_{ns}(q, \dot{q}) < 0\}. \tag{5}$$

Impacts occur when the non-stance foot hits the ground. The post-impact states, computed in terms of pre-impact states, are given by [14]:

$$\Delta_{\mathbf{ss}\to\mathbf{ds}}(q, \dot{q}) = \begin{bmatrix} \mathcal{R}\Delta_q q \\ \mathcal{R}\Delta_{\dot{q}}(q)\dot{q} \end{bmatrix}, \tag{6}$$

where $\mathcal{R}$ is the relabeling matrix required to swap the stance and non-stance legs after impacts.

Model Dynamics. The dynamics of the system can be obtained from the Eular-Lagrange equation of the "unpinned" model, so that the holonomic constraints are used to describe the interaction between the robot and the world for different

domains. Consider the holonomic constraints for a domain $v \in V$, $h_v(q) = 0$ with $h_v(q) \in \mathbb{R}^{n_c^v}$, where n_c^v is the number of constrained degrees of freedom fo the domain v. Then the dynamics of the model can be written as,

$$D(q)\ddot{q} + H(q,\dot{q}) = Bu + J_v^T(q)F_v, \tag{7}$$

where $D(q)$ is the inertia matrix, $H(q,\dot{q})$ is the vector containing the Coriolis and gravity terms, $B \in \mathbb{R}^{n \times n_u}$ is the distribution matrix for the actuators $u \in \mathcal{U} \subset \mathbb{R}^{n_u}$ where n_u is the number of actuators in the system, $J_v(q)$ is the Jacobian of the holonomic constraints for a domain $v \in V$ and $F_v \in \mathbb{R}^{n_c^v}$ are the reaction forces due to the holonomic constraints. For the double support domain, the reaction forces consist of the horizontal and vertical reaction forces on both feet, i.e., $F_{\mathbf{ds}} = (F_s, F_{ns}) \in \mathbb{R}^4$, and for the single support domain, the reaction forces include only the forces on the stance foot, $F_{\mathbf{ss}} = F_s \in \mathbb{R}^2$. For the constraint forces to be valid, the following constraints need to be satisfied [22], [16],

$$\dot{J}_v(q,\dot{q})\dot{q} + J_v(q)\ddot{q} = 0, \tag{8}$$

$$\mathscr{R}_v F_v \geq 0, \tag{9}$$

where $\mathscr{R}_v F_v$ corresponds to a set of admissible constraints that guarantee the physical validity of the model, e.g. positive normal force and friction cone. To formulate the above constraints in the quadratic program, which will be explained in detail later in the paper, we write (7) as

$$D(q)\ddot{q} + H(q,\dot{q}) = \underbrace{\begin{bmatrix} B & J_v^T(q) \end{bmatrix}}_{\bar{B}_v(q)} \underbrace{\begin{bmatrix} u \\ F_v \end{bmatrix}}_{\bar{u}_v}, \tag{10}$$

with $\bar{u}_v \in \mathbb{R}^{n_u + n_c^v}$. With $x = [q, \dot{q}]^T$ as the states of the system, the affine control system is defined based on (10),

$$\dot{x} = f(x) + g_v(x)\bar{u}_v, \tag{11}$$

where

$$f(x) = \begin{bmatrix} \dot{q} \\ -D^{-1}(q)H(q,\dot{q}) \end{bmatrix}, g_v(x) = \begin{bmatrix} 0 \\ D^{-1}(q)\bar{B}_v(q) \end{bmatrix}.$$

III. Embedding of ES-SLIP Dynamics

In this section, we begin by briefly discussing the SLIP walking model and stable walking gait generation. Then we present the motivation of the dynamics embedding controller for the full order dynamics. The remainder of the section focuses on the derivation of desired reduced order dynamics by introducing the energy-stabilizing controller.

SLIP Model. The Spring Loaded Inverted Pendulum (SLIP) model provides a low-dimensional representation of locomotion by utilizing an energy-conserving spring mass model. As such, it can provide an approach for generating efficient gaits on bipedal robots [8], [20]. The spring-mass model consists of a point mass m supported by two massless linear spring legs with fixed rest length r_0 and stiffness k. The spring forces only act on the mass while in contact with the ground and cannot apply forces during swing. Letting p_{com} be the position of the point mass with respect to a fixed origin, the dynamics of the SLIP model is given as follows,

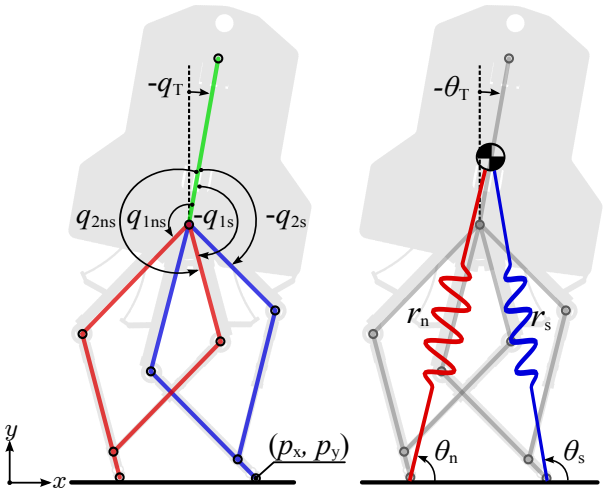

(a) Robot Configuration (b) Outputs

Fig. 3: The coordinate configuration of the robot.

$$\ddot{p}_{com} = \frac{1}{m}\left(F_R(r) + F_L(r)\right) - g, \tag{12}$$

where F_R and F_L are the spring forces of the legs and g is the gravitational vector.

The SLIP walking model consists of two different dynamical phases: single support and double support, identified by the contact constraints of the system. A stable walking gait can be obtained by selecting a proper "touch down" angle, α_{TD}, as shown in Fig. 1. Since the legs are assumed to be massless and controlling them does not require any net actuator work, the system conserves energy. The dynamic stability of a gait is verified through the Poincaré return map for a single step. To be dynamically stable, the magnitudes of all the eigenvalues of the Jacobian matrix of the discrete Poincaré map must be less than 1.

In this paper, we use model parameters that roughly approximate the low-dimensional dynamics of ATRIAS. Stable walking gaits for the given parameters are generated by utilizing the method introduced in [20], and the desired "touch down" angles are determined correspondingly.

Dynamics Embedding. The motivation of the dynamics embedding controller comes from the input/output linearization of a nonlinear system. Rather than defining reference trajectories for the system, we can enforce the output dynamics of the system to be the dynamics of the reduced order model, such that the former exhibits similar dynamical behavior to the latter. In particular, to achieve the SLIP dynamics on ATRIAS, let $y_c = h_c(q)$ be the CoM position of ATRIAS. Differentiating it twice yields

$$\ddot{y}_c = \mathcal{L}_f^2 h_c(q,\dot{q}) + \mathcal{L}_{g_v}\mathcal{L}_f h_c(q,\dot{q})\bar{u}_v, \tag{13}$$

where $\mathcal{L}$ represents the Lie derivative. In the context of feedback linearization, one would pick the output dynamics $\ddot{y}_c = \mu_c$ as a stable linear system such that a corresponding

feedback control law drives the outputs to zero. If, instead, the goal is to drive the output dynamics to a reduced order nonlinear system, e.g. the SLIP model, picking

$$\mu_c = \frac{1}{m}\left(F_R(q,\dot{q}) + F_L(q,\dot{q})\right) - g, \tag{14}$$

yields $\ddot{y}_c = \ddot{p}_{com}$. To achieve this objective, the controller is required to satisfy the following equality constraint

$$A^{\text{SLIP}}\bar{u}_v = (-\mathcal{L}_f^2 h_c(q,\dot{q}) + \ddot{p}_{com}), \tag{15}$$

where $A^{\text{SLIP}} = \mathcal{L}_{g_v}\mathcal{L}_f h_c(q,\dot{q})$ is the decoupling matrix. With this constraint, the controller renders the output dynamics exactly as the corresponding SLIP dynamics.

SLIP Dynamics. To achieve the above goal, we need to explicitly derive the expression for the SLIP dynamics in terms of ATRIAS's states. Consider the whole system as a point mass, m, at its CoM position, and assume virtual massless spring legs attached to the point mass, as shown in Fig. 3. We use the polar coordinates for this purpose; let $X_v = (r_v, \theta_v, \dot{r}_v, \dot{\theta}_v)$ be the states of the SLIP model for domain $v \in V$. For double support phase, we set the front leg as the stance leg and consequently the stance toe as the origin of the coordinates. Then, the desired SLIP dynamics are given in terms of robot states by

$$\ddot{r}_{\mathbf{ds}} = \frac{k}{m}\left(\Delta r_s + \Delta r_n \cos(\theta_s - \theta_n)\right) + r_s\dot{\theta}_s^2 - g\sin\theta_s, \tag{16}$$

$$\ddot{\theta}_{\mathbf{ds}} = -\frac{\frac{k}{m}(\Delta r_n \sin(\theta_s - \theta_n)) + 2\dot{r}_s\dot{\theta}_s + g\cos\theta_s}{r_s}, \tag{17}$$

where $\Delta r_s = (r_0 - r_s)$, $\Delta r_n = (r_0 - r_n)$, r_s and θ_s are the stance virtual leg length and leg angle, and r_n and θ_n are the non-stance virtual leg length and leg angle respectively, as shown in Fig. 3 (b). Note that the virtual leg lengths and leg angles are nonlinear functions of the states $(q,\dot{q})$ of ATRIAS.

Since only the stance leg forces act on the system for the single support domain, the terms due to the non-stance leg spring force will disappear in the dynamics equation. The governing equations of motion are given as

$$\ddot{r}_{\mathbf{ss}} = \frac{k}{m}(\Delta r_s + r_s\dot{\theta}_s^2 - g\sin\theta_s), \tag{18}$$

$$\ddot{\theta}_{\mathbf{ss}} = -\frac{1}{r_s}(2\dot{r}_s\dot{\theta}_s + g\cos\theta_s). \tag{19}$$

It is important to note that the above equations are obtained under the assumption of the energy-conservative SLIP model. However, the total energy of the actual robot system is not constant over a gait, which requires compensation through the input of energy to stabilize the system.

Energy-Stabilized Controller. The existence of compliant legs in the SLIP model ensures the total energy is conserved throughout the impacts. However, the plastic impacts of the actual robot cause energy loss in the system. In [11], an energy-stabilizing controller is introduced to compensate for the energy loss of the system by adding an additional compensation force to the SLIP dynamics discussed previously. Let E_d be the desired energy level and E the actual energy of the reduced order system, then the compensating forces in the radial and angular directions are given by

$$F_c^r = -k_c\frac{\dot{r}_s}{\dot{r}_s^2 + r_s^2\dot{\theta}_s^2}\Delta E, \;\; F_c^\theta = -k_c\frac{r_s\dot{\theta}_s}{\dot{r}_s^2 + r_s^2\dot{\theta}_s^2}\Delta E, \tag{20}$$

where $k_c > 0$ is positive gain and $\Delta E = E - E_d$. Note that the direction of the compensating force is always in the opposite direction of the center of mass velocity. Intuitively, this force is trying to impede the velocity changes due to the energy loss to stabilize the total energy of the system to the desired level.

With these compensating forces in hand we modify the desired SLIP dynamics by adding the following energy-stabilizing controller to obtain the Energy-Stabilized SLIP (ES-SLIP) dynamics for each domain $v \in V$:

$$\ddot{\bar{r}}_v = \ddot{r}_v + F_c^r/m, \quad \ddot{\bar{\theta}}_v = \ddot{\theta}_v + F_c^\theta/m, \tag{21}$$

where F_c^r and F_c^θ are the radial and angular direction components of the Energy-Stabilized forces in (20).

It is possible to easily implement ES-SLIP dynamics on fully-actuated robots. However, in the case of underactuated robots, it is difficult to track the dynamics of ES-SLIP model precisely due to the underactuation. Becuase the ES-SLIP dynamics determine only the motion of the CoM position, other control objectives must be determined in addition to the dynamics embedding controller.

IV. Torso and Non-Stance Leg Control

In order to fully regulate the motion of the robot, we also need to determine additional control tasks, such as the torso and non-stance leg motion. We begin by introducing additional control tasks for the system in general, then specifying tasks for each domain independently.

RES-CLF Construction. For each domain, $v \in V$, we consider the outputs $y_v : \mathcal{Q} \to \mathbb{R}^{n_\ell}$, where n_ℓ is the number of outputs of the system, with the objective of driving $y_v(q) \to 0$. Since the outputs being considered are only functions of the configuration of the robot, differentiating the outputs twice yields

$$\ddot{y}_v = \underbrace{\mathcal{L}_f^2 y(q,\dot{q})}_{(\mathcal{L}_f^2)_v} + \underbrace{\mathcal{L}_{g_v}\mathcal{L}_f y(q,\dot{q})}_{\mathcal{A}_v}\bar{u}_v. \tag{22}$$

Assume that the decoupling matrix, $\mathcal{A}_v$, is well-defined and has full rank [15], i.e., that y_v satisfies the vector relative degree condition (normally vector relative degree two) and consists of linearly independent entries, then we may produce a feedback control law,

$$\bar{u}_v = \mathcal{A}_v^+\left(-(\mathcal{L}_f^2)_v + \mu_v\right), \tag{23}$$

that realizes $\ddot{y}_v = \mu_v$, where $\mathcal{A}_v^+$ is the pseudo inverse of the decoupling matrix. Next, one chooses μ_v so that the resulting output dynamics are stable. Letting $\eta_v = (y_v, \dot{y}_v) \in \mathbb{R}^{2n_\ell}$, the linear output dynamics can be written as

$$\dot{\eta}_v = \underbrace{\begin{bmatrix} 0 & I \\ 0 & 0 \end{bmatrix}}_{F_v}\eta_v + \underbrace{\begin{bmatrix} 0 \\ I \end{bmatrix}}_{G_v}\mu_v. \tag{24}$$

Then in the context of this control system, we consider the continuous time algebraic Riccati equations (CARE):

$$F_v^T P_v + P_v F_v - P_v G_v G_v^T P_v + Q_v = 0, \tag{25}$$

for $Q_v = Q_v^T > 0$ with solution $P_v = P_v^T > 0$. One can use P_v to construct a RES-CLF that can be used to exponentially stabilize the output dynamics at a user defined rate of $\frac{1}{\varepsilon}$ (see [4], [5]). In particular, define

$$V_v^\varepsilon(\eta_v) = \eta_v^T \underbrace{I^\varepsilon P_v I^\varepsilon}_{P_v^\varepsilon} \eta_v, \qquad \text{with} \quad I^\varepsilon = \operatorname{diag}(\frac{1}{\varepsilon} I, I), \tag{26}$$

wherein it follows that:

$$\dot{V}_v^\varepsilon(\eta_v) = \mathcal{L}_{F_v} V_v^\varepsilon(\eta_v) + \mathcal{L}_{G_v} V_v^\varepsilon(\eta_v)\mu_v,$$

with

$$\begin{aligned} \mathcal{L}_{F_v} V_v^\varepsilon(\eta_v) &= \eta_v^T (F_v^T P_v^\varepsilon + P_v^\varepsilon F_v)\eta_v, \\ \mathcal{L}_{G_v} V_v^\varepsilon(\eta_v) &= 2\eta_v^T P_v^\varepsilon G_v. \end{aligned} \tag{27}$$

With the goal of exponentially stabilizing the η_v to zero, we wish to find μ_v such that,

$$\mathcal{L}_{F_v} V_v^\varepsilon(\eta_v) + \mathcal{L}_{G_v} V_v^\varepsilon(\eta_v)\mu_v \leq -\frac{\gamma}{\varepsilon} V_v^\varepsilon(\eta_v),$$

for some $\gamma > 0$. In particular, it allows for specific feedback controllers, e.g., the min-norm controller, which can be stated as the closed form solution to a quadratic program (QP). See [6], [5] for the further information.

Recalling that $\mathcal{A}_v \bar{u}_v = -(\mathcal{L}_f^2)_v + \mu_v$, it follows that:

$$\mu_v^T \mu_v = \bar{u}_v^T \mathcal{A}_v^T \mathcal{A}_v \bar{u}_v + 2(\mathcal{L}_f^2)_v^T \mathcal{A}_v \bar{u}_v + (\mathcal{L}_f^2)_v^T (\mathcal{L}_f^2)_v,$$

which allows for reformulating the QP problem in terms of $\bar{u}_v$ instead of μ_v, so that additional constraints on torques or reaction forces can be directly implemented in the formulation. To achieve an optimal control law, we can relax the CLF constraints and penalize this relaxation. In particular, we consider the following modified CLF-based QP in terms of $\bar{u}_v$ and a relaxation factor δ_v:

$$\underset{(\bar{u}_v, \delta_v) \in \mathbb{R}^{n_u + n_c^v + 1}}{\operatorname{argmin}} \quad p_v \delta_v^2 + \bar{u}_v^T \mathcal{A}_v^T \mathcal{A}_v \bar{u}_v + 2(\mathcal{L}_f^2)_v^T \mathcal{A}_v \bar{u}_v \tag{28}$$

$$\text{s.t} \qquad \tilde{A}_v^{\text{CLF}}(q, \dot{q})\bar{u}_v \leq \tilde{b}_v^{\text{CLF}}(q, \dot{q}) + \delta_v \quad \text{(CLF)}$$

where,

$$\begin{aligned} \tilde{A}_v^{\text{CLF}}(q, \dot{q}) :=& \mathcal{L}_{G_v} V_v^\varepsilon(q, \dot{q}) \mathcal{A}_v(q, \dot{q}), \\ \tilde{b}_v^{\text{CLF}}(q, \dot{q}) :=& -\frac{\gamma}{\varepsilon} V_v^\varepsilon(q, \dot{q}) - \mathcal{L}_{F_v} V_v^\varepsilon(q, \dot{q}) \\ & - \mathcal{L}_{G_v} V_v^\varepsilon(q, \dot{q})(\mathcal{L}_f^2)_v, \end{aligned} \tag{29}$$

and $p_v > 0$ is a large positive constant that penalizes violations of the CLF constraint. Note that we use the fact that η_v is a function of the system states $(q, \dot{q})$, so the constraints can be expressed in the term of system states.

The end result of solving this QP is the optimal control law that guarantees exponential convergence of the control objective $y_v \to 0$ if $\delta_v \equiv 0$. In the case of sufficiently small δ_v, we still achieve exponential convergence of the outputs, which motivates the minimization of δ_v in the cost of QP.

Outputs Definition. With the construction of RES-CLFs in hand, now we specify the outputs for each domain independently.

Double Support Domain. Since both the stance and non-stance legs are constrained during the double support domain, we only consider the torso angle θ_T in addition to the dynamics embedding controller. In particular, the outputs for the *double support* domain are defined as the error between the actual outputs and desired outputs,

$$y_{\mathbf{ds}} = \theta_T - y_H(t, \alpha_{torso}), \tag{30}$$

where $\theta_T = q_T$ as shown in Fig. 3(b). The desired outputs are characterized by a smooth function, called the *canonical walking function*, defined to be the time solution to a mass-spring-damper system,

$$y_H(t, \alpha) = e^{-\alpha_4 t}(\alpha_1 \cos(\alpha_2 t) + \alpha_3 \sin(\alpha_2 t)) + \alpha_5. \tag{31}$$

Note that the justification of this function form can be found in [3]. α_{torso} is the corresponding parameters vector of the torso output.

Single Support Domain. The robot becomes an underactuated system in the single support domain, which increases the difficulty of determining the control task for this domain. First, to move the non-stance leg forward during stance, we need to define at least two outputs related to the non-stance leg. Also, ATRIAS has a relatively heavy torso, therefore the torso angle has to be considered in the outputs to stabilize the system effectively. Since the system has only four actuators, we have to loosen the requirement for dynamics embedding, which we will present in detail in Sect. V. Picking the nonlinear virtual leg length and leg angle (r_n, θ_n) (see Fig. 3(b)) that represent the motion of the non-stance leg, the outputs for the single support domain are defined as

$$y_{\mathbf{ss}} = \underbrace{\begin{bmatrix} \theta_T(q) \\ r_n(q) \\ \theta_n(q) \end{bmatrix}}_{y_{\mathbf{ss}}^a} - \underbrace{\begin{bmatrix} y_H(t, \alpha_{torso}) \\ y_H(t, \alpha_{r_n}) \\ y_H(t, \alpha_{\theta_n}) \end{bmatrix}}_{y_{\mathbf{ss}}^d}, \tag{32}$$

where α_{r_n} and α_{θ_n} are the parameter vectors of the non-stance leg outputs. To ensure a feasible walking gait, those parameters are chosen such that the touch-down angle requirement from the SLIP gait is achieved. Also α_{torso} are picked with the goal of keeping the torso angle at almost a constant value.

With the definition of the outputs for each domain, the corresponding RES-CLF constraints for each domain can be constructed from (29) to formulate the objective of the torso and non-stance leg control in the quadratic program discussed in the next section.

V. Main Control Law

In this section, we present a multi-objective quadratic program based control law which simultaneously embeds the ES-SLIP dynamics into the full-order robot system

and achieves convergence of the additional control objectives. Control values are obtained through the solution of a quadratic program with linear constraints. Specifically, we use the ES-SLIP embedding equation from Sect. III and the RES-CLF convergence inequality from Sect. IV to construct constraints which are affine in $\bar{u}_v$. Within this framework, we also include constraints on the full order robot dynamics, such as ground reaction force constraints and actuator torque limits.

The main objective of the proposed controller is to drive the low-dimensional representation computed on the full-order dynamics to be as close to the ES-SLIP behavior as possible. To realize this goal, three sub-objectives must be met: the dynamics of the full-order robot's CoM must match those of the ES-SLIP, the domain switches must occur at the same state, and the swing-leg outputs must match. These three objectives are encoded into the proposed controller through linear constraints on $\bar{u}_v$.

SLIP Dynamics Constraints. As the robot is fully actuated in the double support domain, we can completely embed the ES-SLIP dynamics into the full order system. To achieve the ES-SLIP dynamics on the full robot dynamics, define the following equality constraints:

$$A^{\text{SLIP}}_{\mathbf{ds}}(q,\dot{q}) := \mathcal{L}_{g_{\mathbf{ds}}}\mathcal{L}_f h_c(q,\dot{q}), \tag{33}$$

$$b^{\text{SLIP}}_{\mathbf{ds}}(q,\dot{q}) := \ddot{y}^c_{\mathbf{ds}} - \mathcal{L}_f^2 h_c(q,\dot{q})), \tag{34}$$

where $\ddot{y}^c_{\mathbf{ds}} := (\ddot{\tilde{r}}_{\mathbf{ds}}, \ddot{\tilde{\theta}}_{\mathbf{ds}})$ are the dynamics of the ES-SLIP model as defined in (21) in the case of $v = \mathbf{ds}$. and $h_c(q,\dot{q}) := (r_s, \theta_s)$ is the CoM position of ATRIAS in polar coordinates.

As discussed in the previous section, the requirement for the dynamics embedding must be reformulated for the single support domain for underactuated robots. Inspired by the fact that the spring force due to deflection of stance leg length is the only force, aside from gravity, acting on the CoM in the SLIP model, we propose an alternative partial embedding controller in this paper. More specifically, instead of matching the CoM acceleration in both coordinates, we only enforce acceleration matching in the radial, i.e. virtual leg length direction. Therefore, for the single support domain, define the partial dynamics embedding constraints as follows:

$$A^{\text{SLIP}}_{\mathbf{ss}}(q,\dot{q}) := \mathcal{L}_{g_{\mathbf{ss}}}\mathcal{L}_f r_s(q,\dot{q}), \tag{35}$$

$$b^{\text{SLIP}}_{\mathbf{ss}}(q,\dot{q}) := \ddot{\tilde{r}}_{\mathbf{ss}} - \mathcal{L}_f^2 r_s(q,\dot{q})), \tag{36}$$

where $\ddot{\tilde{r}}_{\mathbf{ss}}$ is given in (21) in the case of $v = \mathbf{ss}$.

Reaction Force Matching Constraints. During the double support phase, additional constraints are needed to ensure that the reaction forces on the two legs are closer to the corresponding forces of the SLIP model, i.e., so the full order model displays similar transitions from double support to single support. Exactly matching the reaction forces on both legs will over constrain the QP due to the difference between the full order model and the reduced order model. Hence we only constrain the reaction forces on the non-stance leg as it determine the switching behavior of ATRIAS. Letting n_σ be the number of forces that will be matched with a desired force, where in this case $n_\sigma = 2$, we define the following inequality constraints:

$$|F_{ns} - F^{\text{SLIP}}_{ns}| \leq \sigma,$$

where $F^{\text{SLIP}}_{ns} \in \mathbb{R}^{n_\sigma}$ is the equivalent spring force of the non-stance leg of the SLIP model computed in terms of system state. With the goal of minimizing σ, we add it to the cost function of the QP, and define,

$$A^{\text{SLIP}}_F(q,\dot{q}) := \begin{bmatrix} \mathbf{0}_{n_\sigma \times (n_u + n_c^{\mathbf{ds}} - n_\sigma)} & I_{n_\sigma \times n_\sigma} \\ \mathbf{0}_{n_\sigma \times (n_u + n_c^{\mathbf{ds}} - n_\sigma)} & -I_{n_\sigma \times n_\sigma} \end{bmatrix}, \tag{37}$$

$$b^{\text{SLIP}}_F(q,\dot{q}) := \begin{bmatrix} F^{\text{SLIP}}_{ns} \\ -F^{\text{SLIP}}_{ns} \end{bmatrix}. \tag{38}$$

Full Robot Model Constraints. In addition to realizing ES-SLIP behavior in the full-order robot dynamics, the control values obtained through the quadratic program must also be in the set of admissible control values, as determined by the full-order robot model.

Torque Constraints. To ensure that the solution to the quadratic program is within the feasible limits of the hardware, define the following torque constraints:

$$A^\tau_v(q,\dot{q}) = \begin{bmatrix} I_{n_u \times n_u} & \mathbf{0}_{n_u \times n_c^v} \\ -I_{n_u \times n_u} & \mathbf{0}_{n_u \times n_c^v} \end{bmatrix}, b^\tau_v(q,\dot{q}) = \begin{bmatrix} \tau_{\max}\mathbf{1}_{n_u} \\ -\tau_{\min}\mathbf{1}_{n_u} \end{bmatrix}.$$

Reaction-Force Constraints. To ensure admissibility of the reaction forces, such as positive normal forces and a no-slipping condition, define the constraints based on (9):

$$A^F_v(q,\dot{q}) = \begin{bmatrix} \mathbf{0}_{n_c^v \times n_u} & -\mathscr{R}_v \end{bmatrix}, \quad b^F_v(q,\dot{q}) = \mathbf{0}_{n_c^v}. \tag{39}$$

Holonomic (Ground-Contact) Constraints. To keep the feet pinned, define the following constraints enforcing (8):

$$\begin{aligned} Aeq^F_v(q,\dot{q}) &= J_v(q)D(q)^{-1}\bar{B}_v(q), \\ beq^F_v(q,\dot{q}) &= J_v(q)D(q)^{-1}H(q,\dot{q}) - \dot{J}_v(q,\dot{q})\dot{q}. \end{aligned} \tag{40}$$

Quadratic Program Formulation. Utilizing the constructions presented above, we now present the main result of the paper. The CLF-based QP for each domain is formulated explicitly formulated as follows:

Double-Support QP. Let $(\bar{u}^*_{\mathbf{ds}}, \delta^*_{\mathbf{ds}}, \sigma^*) \in \mathbb{R}^{n_{\mathbf{ds}}}$ with $n_{\mathbf{ds}} = 1 + n_u + n_c^{\mathbf{ds}} + n_\sigma$; the final form of the QP problem for the double support domain is given as

$$\begin{aligned} \underset{(\bar{u}_{\mathbf{ds}}, \delta_{\mathbf{ds}}, \sigma) \in \mathbb{R}^{n_{\mathbf{ds}}}}{\operatorname{argmin}} \quad & p_{\mathbf{ds}}\delta^2_{\mathbf{ds}} + \bar{u}^T_{\mathbf{ds}}\mathcal{A}^T_{\mathbf{ds}}\mathcal{A}_{\mathbf{ds}}\bar{u}_{\mathbf{ds}} \qquad \text{(DS-QP)} \\ & + 2(\mathcal{L}^2_f)^T_{\mathbf{ds}}\mathcal{A}_{\mathbf{ds}}\bar{u}_{\mathbf{ds}} + p_\sigma \sigma^T\sigma \\ \text{s.t.} \quad & A^{\text{SLIP}}_{\mathbf{ds}}(q,\dot{q})\bar{u}_{\mathbf{ds}} = b^{\text{SLIP}}_{\mathbf{ds}}(q,\dot{q}) \qquad \text{(SLIP)} \\ & A^{\text{SLIP}}_F(q,\dot{q})\bar{u}_{\mathbf{ds}} \leq b^{\text{SLIP}}_F(q,\dot{q}) + \sigma \qquad \text{(SLIP-Force)} \\ & \tilde{A}^{\text{CLF}}_{\mathbf{ds}}(q,\dot{q})\bar{u}_{\mathbf{ds}} \leq \tilde{b}^{\text{CLF}}_{\mathbf{ds}}(q,\dot{q}) + \delta_{\mathbf{ds}} \qquad \text{(RES-CLF)} \\ & A^F_{\mathbf{ds}}(q,\dot{q})\bar{u}_{\mathbf{ds}} \leq b^F_{\mathbf{ds}}(q,\dot{q}) \qquad \text{(Contact Forces)} \\ & A^\tau_{\mathbf{ds}}(q,\dot{q})\bar{u}_{\mathbf{ds}} \leq b^\tau_{\mathbf{ds}}(q,\dot{q}) \qquad \text{(Torque)} \\ & Aeq^F_{\mathbf{ds}}(q,\dot{q})\bar{u}_{\mathbf{ds}} = beq^F_{\mathbf{ds}}(q,\dot{q}) \qquad \text{(Constraints)} \end{aligned}$$

where $p_\sigma > 0$ is a large positive constant that penalizes violations of the SLIP force constraints.

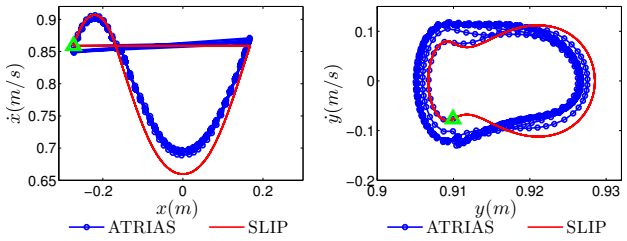

Fig. 4: The phase portrait comparison of the CoM dynamics between the equilibrium SLIP gait and the ATRIAS walking gait.

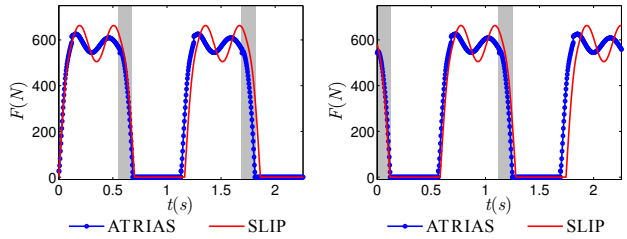

(a) Right Leg (b) Left Leg

Fig. 5: Comparison of the ground reaction force along the leg length direction between the ideal SLIP gait and the full-order robotic model.

Single-Support QP. Let $(\bar{u}^*_{\mathbf{ss}}, \delta^*_{\mathbf{ss}}) \in \mathbb{R}^{n_{\mathbf{ss}}}$ with $n_{\mathbf{ss}} = 1 + n_u + n_c^{\mathbf{ss}}$; the final form of the QP problem for the double support domain is given as

$$\underset{(\bar{u}_{\mathbf{ss}}, \delta_{\mathbf{ss}}) \in \mathbb{R}^{n_{\mathbf{ss}}}}{\operatorname{argmin}} \quad p_{\mathbf{ss}}\delta_{\mathbf{ss}}^2 + \bar{u}_{\mathbf{ss}}^T \mathcal{A}_{\mathbf{ss}}^T \mathcal{A}_{\mathbf{ss}} \bar{u}_{\mathbf{ss}} + 2(\mathcal{L}_f^2)_{\mathbf{ss}}^T \mathcal{A}_{\mathbf{ss}} \bar{u}_{\mathbf{ss}} \qquad \text{(SS-QP)}$$

$$\begin{aligned}
\text{s.t.} \quad & A_{\mathbf{ss}}^{\text{SLIP}}(q,\dot{q})\bar{u}_{\mathbf{ss}} = b_{\mathbf{ss}}^{\text{SLIP}}(q,\dot{q}) && \text{(SLIP)} \\
& \tilde{A}_{\mathbf{ss}}^{\text{CLF}}(q,\dot{q})\bar{u}_{\mathbf{ss}} \leq \tilde{b}_{\mathbf{ss}}^{\text{CLF}}(q,\dot{q}) + \delta_{\mathbf{ss}} && \text{(RES-CLF)} \\
& A_{\mathbf{ss}}^{F}(q,\dot{q})\bar{u}_{\mathbf{ss}} \leq b_{\mathbf{ss}}^{F}(q,\dot{q}) && \text{(Contact Forces)} \\
& A_{\mathbf{ss}}^{\tau}(q,\dot{q})\bar{u}_{\mathbf{ss}} \leq b_{\mathbf{ss}}^{\tau}(q,\dot{q}) && \text{(Torque)} \\
& Aeq_{\mathbf{ss}}^{F}(q,\dot{q})\bar{u}_{\mathbf{ss}} = beq_{\mathbf{ss}}^{F}(q,\dot{q}) && \text{(Constraints)}
\end{aligned}$$

We apply the feedback control law $\bar{u}_{\mathbf{ds}}$ and $\bar{u}_{\mathbf{ss}}$ obtained from the result of (DS-QP) and (SS-QP) to the hybrid control system (11), to get a set of feedback vector fields $F = \{\bar{f}_{\mathbf{ds}}, \bar{f}_{\mathbf{ss}}\}$, which yields the closed-form hybrid system:

$$\mathscr{H} = (\Gamma, \mathcal{D}, S, \Delta, F), \qquad (41)$$

where Γ, $\mathcal{D}$, S and Δ are defined as for $\mathscr{HC}$ in (1).

VI. Simulation Results

In this section we present the simulation results on ATRIAS to demonstrate the effectiveness of the control law obtained from Sect. V. We compare the resulting dynamical behaviors of ATRIAS with the ones of the SLIP model. The convergence and existence of the limit cycles show the stability of the control system with the proposed control law.

Dynamic Matching Behavior. To show the analog between the SLIP dynamics and ATRIAS's' dynamics, we perform a simulation of the full order system starting from the same post impact states as the equilibrium SLIP gait. Fig. 4 shows the phase portrait comparison of the CoM dynamics between both the full and reduced order system. The triangle point indicates the initial condition of both systems. As shown in the figure, the dynamics of ATRIAS exactly follow the ones of the SLIP model during the first double support domain, then deviate from the SLIP dynamics when switched to the single support domain, and ultimately converge to a limit cycle, which can be seen from the density of the dotted lines, that are different from the SLIP gait limit cycle. That is because we only apply partial embedding of the dynamics during the single support domain. Although the ATRIS gait dynamics do not exactly match the SLIP dynamics, the overall behavior is very similar to the SLIP gait. The comparisons of CoM positions and velocities between stable ATRIAS gait and equilibrium gait over four steps in Fig. 8 show such similarities very clearly.

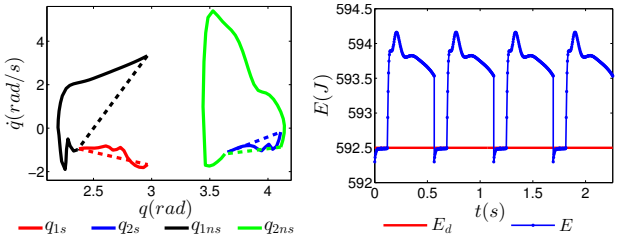

(a) Limit Cycles (b) Energy

Fig. 6: Limit cycle and Energy convergence of the stable walking gait of four steps obtained in the full order model.

Enforcing the proposed constraints in (37) ensures that reaction forces on the non-stance foot match the SLIP spring forces, as shown in Fig. 5. Note that the plots are shown in terms of the right and left leg, instead of stance/non-stance legs. The gray areas in the plots indicate the regions where the constraints are imposed. It is also interesting to note that the reaction forces on the stance foot are also very close to the corresponding virtual spring forces without explicitly imposing a constraint on their equality.

System Stability. As we noticed in Fig. 4, the CoM states converge to a limit cycle after approximately 8 steps. The stability of the control system is further verified with the existence of the limit cycle. Fig. 6a shows the limit cycle of the full order system. The simulation results show that the system states converge to the limit cycle exponentially. The energy of the full order system also is stabilized with the use of ES-SLIP. Unlike the SLIP model, the total energy of the full order system, shown in Fig. 6b, is not conserved as we can only enforce partial COM dynamics behavior during underaction. The energy slightly deviates from the desired energy level during the single support, but still exponentially converges to the desired level in the double support domain.

A numerical verification using the Poincaré return map is also performed, with the pre-impact instant as the Poincaré section of the system. The maximum eigenvalue of linearized

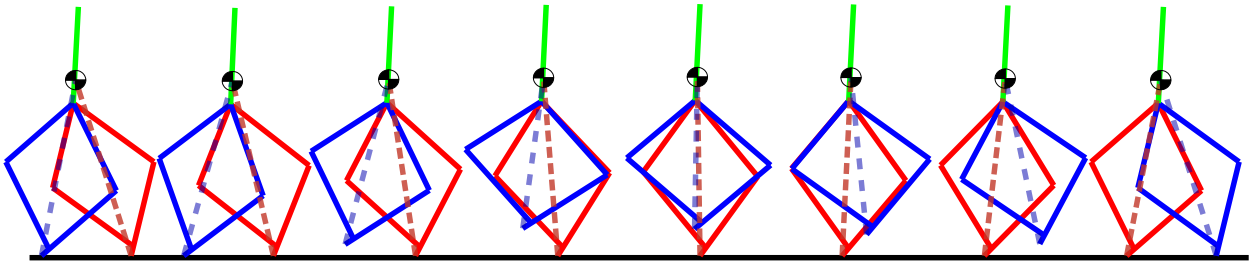

Fig. 7: The walking gait snapshot of ATRIAS over one step.

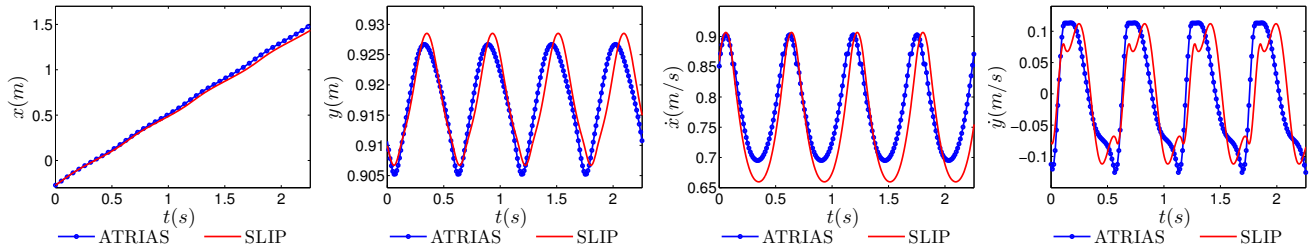

(a) Horizontal Position (b) Vertical Position (c) Horizontal Velocity (d) Vertical Velocity

Fig. 8: Comparison of CoM position and velocity of stable walking gait vs equilibrium SLIP gait.

dynamics at the Poincaré section is $\lambda_{max} \approx 0.71 < 1$, which shows the stability of the resulting walking gait. Snapshots of one step of the stable walking gait is shown in Fig. 7.

ACKNOWLEDGMENT

The authors would like to thank Jonathan Hurst and the OSU Dynamic Robotic Laboratory for the many discussions on SLIP walking and its importance in robot locomotion. This research is supported by SRI International and NSF grant CPS-1239055.

REFERENCES

[1] Sustained walking of ATRIAS 2.1: http://youtu.be/yiEbWwC-sR0.

[2] R. Altendorfer, D. E. Koditschek, and P. Holmes. Stability analysis of legged locomotion models by symmetry-factored return maps. *International Journal of Robotics Research*, 23(10-11):979–999, 2004.

[3] A. D. Ames. First steps toward underactuated human-inspired bipedal robotic walking. In *2012 IEEE International Conference on Robotics and Automation (ICRA)*, pages 1011–1017, May 2012.

[4] A. D. Ames, K. Galloway, and J. W. Grizzle. Control lyapunov functions and hybrid zero dynamics. In *2012 IEEE 51st Annual Conference on Decision and Control (CDC)*, pages 6837–6842, Dec 2012.

[5] A. D. Ames, K. Galloway, K. Sreenath, and J. W. Grizzle. Rapidly exponentially stabilizing control lyapunov functions and hybrid zero dynamics. *IEEE Transactions on Automatic Control (TAC)*, 59(4):876–891, April 2014.

[6] A. D. Ames and M. J. Powell. Towards the unification of locomotion and manipulation through control lyapunov functions and quadratic programs. In *Control of Cyber-Physical Systems*, pages 219–240. Springer, 2013.

[7] R. Blickhan. The spring-mass model for running and hopping. *Journal of Biomechanics*, 22(11):1217–1227, 1989.

[8] S. Collins, A. Ruina, R. Tedrake, and M. Wisse. Efficient bipedal robots based on passive-dynamic walkers. *Science*, 307(5712):1082–1085, 2005.

[9] R. A. Freeman and P. V. Kokotovic. *Robust nonlinear control design: state-space and Lyapunov techniques*. Springer, 2008.

[10] K. S. Galloway, K. Sreenath, A. D. Ames, and J. W. Grizzle. Torque saturation in bipedal robotic walking through control lyapunov function based quadratic programs. *CoRR*, abs/1302.7314, 2013.

[11] G. Garofalo, C. Ott, and A. Albu-Schaffer. Walking control of fully actuated robots based on the bipedal slip model. In *IEEE International Conference on Robotics and Automation*, pages 1456–1463, 2012.

[12] H. Geyer, A. Seyfarth, and R. Blickhan. Compliant leg behaviour explains basic dynamics of walking and running. *Proceedings of the Royal Society B-Biological Sciences*, 273(1603):2861–2867, NOV 22 2006.

[13] J. A. Grimes and J. W. Hurst. The design of ATRIAS 1.0 a unique monoped, hopping robot. In *International Conference on Climbing and Walking Robots (CLAWAR)*, pages 548–554, 2012.

[14] A. Hereid, S. Kolathaya, M. S. Jones, J. Van Why, J. W. Hurst, and A. D. Ames. Dynamic multi-domain bipedal walking with ATRIAS through slip based human-inspired control. In *Proceedings of the 17th International Conference on Hybrid Systems: Computation and Control (HSCC)*, pages 263–272. ACM, 2014.

[15] S. Kolavennu, S. Palanki, and J. C. Cockburn. Nonlinear control of nonsquare multivariable systems. *Chemical Engineering Science*, 56(6):2103–2110, 2001.

[16] B. Morris, M. J. Powell, and A. D. Ames. Sufficient conditions for the lipschitz continuity of qp-based multi-objective control of humanoid robots. In *2013 IEEE 52nd Annual Conference on Decision and Control (CDC)*, pages 2920–2926, Dec 2013.

[17] I. Poulakakis and J. W. Grizzle. The spring loaded inverted pendulum as the hybrid zero dynamics of an asymmetric hopper. *IEEE Transactions on Automatic Control (TAC)*, 54(8):1779–1793, Aug 2009.

[18] M. H. Raibert. *Legged robots that balance*, volume 3. MIT press Cambridge, MA, 1986.

[19] A. Ramezani, J. W. Hurst, K. A. Hamed, and J. W. Grizzle. Performance analysis and feedback control of ATRIAS, a three-dimensional bipedal robot. *Journal of Dynamic Systems Measurement and Control*, 136(2), Mar 2014.

[20] J. Rummel, Y. Blum, H. M. Maus, C. Rode, and A. Seyfarth. Stable and robust walking with compliant legs. In *2010 IEEE International Conference on Robotics and Automation*, pages 5250–5255, May 2010.

[21] K. Sreenath, H. Park, I. Poulakakis, and J. W. Grizzle. A compliant hybrid zero dynamics controller for stable, efficient and fast bipedal walking on MABEL. *The International Journal of Robotics Research*, 30(9):1170–1193, 2011.

[22] E. R. Westervelt, J. W. Grizzle, C. Chevallereau, J. H. Choi, and B. Morris. *Feedback control of dynamic bipedal robot locomotion*. CRC press Boca Raton, 2007.